Chapter 4

Influence of microscopic particle interaction models on the flux of atmospheric protons & antiprotons

4.1 Introduction

A proton flux deep in the atmosphere results from the production of protons in the interactions of primary/secondary cosmic rays with air nuclei as well as the absorption of such protons during their propagation through the Earth's atmosphere. Secondary proton spectrum at very high altitude is likely to contain cleaner information on proton production alone. As the major fraction of such secondary protons arises from hadronic interactions in the forward kinematic region, a study of such proton spectra at very high altitude is likely to provide us with an opportunity to investigate particle production in the forward region.

Antiprotons ($\bar{p}$) in cosmic rays, on the other hand, are supposed to provide information on the sources of cosmic rays and their propagation in the galaxy as well as the matter-antimatter asymmetry of the local universe [164]. They are also believed to play crucial role in indirect dark matter search [165–167]. Primary $\bar{p}$ may as well be produced from the evaporation of primordial black holes (PBH)

[168, 169]. Observations of $\bar{p}$ spectrum with appropriate features may, therefore, be considered for probing into the possible signatures of the PBH.

Recently, the PAMELA instruments attached to the Russian Resurs-DK1 satellite have made a precise measurement of $\bar{p}$ spectrum in the energy range from 60 MeV to 180 GeV [170, 171]. Comparison with several theoretical estimates [195, 214, 217] seems to support the view that the PAMELA $\bar{p}$ spectrum is consistent with a scenario of pure secondary production of $\bar{p}$ *via.* cosmic ray interactions in the interstellar medium (ISM) [170, 171].

An accurate estimation of the secondary proton/antiproton flux is, however, a difficult task. This is because of the fact that such an estimate requires precise knowledge of three factors, namely, the detailed features of cosmic ray propagation in the Galaxy, the characteristics of high energy particle interactions and the effect of solar modulation on the cosmic rays. While there have been a reasonable understanding of the solar modulation effect, major uncertainties in the predicted flux still arise from our incomplete knowledge of cosmic ray propagation and the high energy particle interactions.

Over the past few years, the BESS experiments have reported the results of the precise measurements of atmospheric $\bar{p}$ spectra in an energy range $0.2-3.4$ GeV at three observation levels, namely, the balloon altitude, mountain altitude and the sea level [51, 224]. It is interesting to note that the cosmic rays traverse a depth $(5-6$ g cm$^{-2})$ of matter in the Galaxy that is close to the average atmospheric depth (10.7 g cm^{-2}) of the BESS-2001 balloon observation at the location of Ft. Sumner, USA [224]. As the $\bar{p}$ production mechanism in the atmosphere is likely to be similar to that in the Galaxy, a study of such atmospheric $\bar{p}$ at balloon altitude would possibly provide us with an opportunity to quantify the uncertainty in the theoretical estimate of interstellar $\bar{p}$ flux that may be caused by our limited knowledge of high energy particle interactions.

A good knowledge of particle interactions in the energy range from sub-GeV to about 100 GeV is required to understand the production and transport of the BESS-detected atmospheric $\bar{p}$s with their energies in the range between 0.2 GeV to a few GeV. Due to the steeply falling energy spectra of the primary cosmic rays, the contribution of primary particles with energies above 80 GeV/n to such BESS-observed atmospheric $\bar{p}$ spectrum has been recently found to be insignificant [189]. GHEISHA (version 2002d) [105], UrQMD (version 1.3) [133, 134] and

FLUKA (version 2008.3b) [135, 136] are among the most popular models for describing particle interactions in the relevant energy range. Such models are useful for the study of the development of cosmic ray cascades in the atmosphere. Among the three models mentioned above, GHEISHA is based on the parametrization of accelerator data, while UrQMD and FLUKA describe particle interactions microscopically.

In this present work, the dependence of atmospheric proton flux at balloon altitude on various hadronic interaction models is examined apart from the study of such a dependence on the atmospheric $\bar{p}$ spectrum through the three dimensional Monte Carlo (MC) simulation methods. For such a purpose, first the atmospheric $\bar{p}$ spectra at multiple observation levels are simulated by using FLUKA and UrQMD models and then compare such simulated spectra with the BESS observations. The interaction model GHEISHA is not considered here (except in Figure 4.2(b) (right)) as the model is known to have shortcoming in describing fixed target accelerator data as well as the atmospheric cosmic ray data [189, 196, 203]. The present study is also prompted by the recently reported fact [189] that the BESS-measured atmospheric $\bar{p}$ flux at mountain altitude [51] is substantially less than the simulated flux obtained from FLUKA, while the flux obtained from UrQMD is consistent with experimental measurements. It is important to know whether such a discrepancy between the simulated and the experimental fluxes persists even at a very high (balloon) altitude or at the sea level. Such a study may have important bearing on our understanding of the reasons behind the disagreement between the FLUKA-derived results and the BESS measurements.

It can be noted that several MC simulations [187, 198, 205, 219, 220], relying mostly on phenomenological description of high energy particle interactions, have been carried out in the past to study the atmospheric $\bar{p}$ spectra. Such an approach does not usually satisfy many of the conservation laws in a single hadronic interaction and also suffers from various other inconsistencies (see, for instance, [190]). Besides, an understanding of the atmospheric $\bar{p}$ production also requires a good estimation of cosmic ray secondaries (mostly protons) in the atmosphere that was not considered in many of such earlier studies. In the present study, the residual effect of the galactic $\bar{p}$ flux at the observation level is further taken into consideration that was mostly ignored in the calculations mentioned above.

The BESS-measured $\bar{p}$ spectra are limited to 3.4 GeV that corresponds to the mean

vertical geomagnetic rigidity cutoff at the location of Ft. Sumner, USA. A simulation study of atmospheric $\bar{p}$ at very high altitude, that corresponds with the BESS observations at Ft. Sumner, is therefore relevant only for the low energy end of the galactic $\bar{p}$ spectrum measured by the PAMELA experiment [170, 171]. To simulate the atmospheric $\bar{p}$ flux up to about 100 GeV, a good understanding of particle interactions up to at least a few hundred GeV is necessary. Due to the paucity of experimental data [197] on the inclusive $\bar{p}$ production and annihilation cross-sections over the whole kinematic region in hadron-hadron, hadron-nucleus and nucleus-nucleus collisions in the stated energy range, one has to strongly rely on various theoretical models of particle interactions. In the absence of experimental data, It is here compare the predictions of the well known high energy interaction models QGSJET (version 01c) [94], VENUS (version 4.12) [106], NEXUS (version 3.97) [127, 128] and EPOS (version 1.6) [107], each in combination with FLUKA (version 2008.3b) for the description of hadronic interactions below 80 GeV/n, to get some idea about the theoretical uncertainties in the predicted $\bar{p}$ flux at energies beyond the upper cutoff for the BESS-2001 balloon experiment, i.e., over an energy range of about $3 - 100$ GeV.

Apart from the ambiguity in high energy particle interactions, a dominant systematic error in evaluating the flux of cosmic ray secondaries arises from the uncertainties involved in the estimation of input fluxes of primary cosmic rays. To minimize such uncertainties, spectra of different primary particles measured by the BESS-98 experiment [50] are used as the inputs in our simulations such that the systematic errors in the calculation of atmospheric fluxes are nearly eliminated as the BESS experimental fluxes of atmospheric protons/antiprotons at different altitudes are compared with.

The plan of this work is outlined as in the following. In the next section, the production mechanisms of $\bar{p}$ in high energy collisions and the ways in which different models implement such mechanisms are described briefly. In Sec. 4.3, a brief description of the adapted simulation technique is given. In Sec. 4.4, the results of our MC simulations are presented. Summary and discussion are presented in Sec. 4.5.

4.2 Production and transport of antiprotons in the atmosphere

4.2.1 General aspects

Antiproton flux in the atmosphere relies mainly on two factors, namely, the inclusive $\bar{p}$ production cross-section in cosmic ray-air nuclei collisions and the propagation of $\bar{p}$ in the atmosphere. The latter factor also includes ionization energy loss, loss of $\bar{p}$ due to annihilation and other interactions.

Antiprotons are produced in the atmosphere in high energy interactions of primary and secondary cosmic ray hadrons/nuclei with air nuclei. A typical example could be the interaction $p + N \rightarrow \bar{p} + p + p + N$ with N representing a nucleon. The threshold proton energy for such interaction is about 6.6 GeV in the rest frame of the target nucleon. In addition to the above interactions, meson-nucleon interactions may also lead to the excitation of color flux tubes and their subsequent decay into baryon-antibaryon pairs.

The final state in high energy hadron-nucleon collisions often consists of many particles. Basic reaction for the production of $\bar{p}$ is, therefore, the inclusive $N + N \rightarrow \bar{p}$ + anything process and the inclusive $\bar{p}$ production cross-section is one of the main ingredients for the calculation of atmospheric $\bar{p}$ flux. Such $\bar{p}$ production is likely to take place in the central kinematic region rather than the fragmentation region. Antibaryon absorption can also be important in the case of massive nuclear collisions. The $\bar{p}$ mean multiplicity is the other main input for the $\bar{p}$ production spectrum. For propagation of $\bar{p}$ through the atmosphere, the annihilation cross-section of $\bar{p}$ due to its collisions on light nuclei (N and O) are of primary importance.

In the instant case, several $\bar{p}$ production cross-section data on the collisions of proton with various fixed target nuclei in the (laboratory) energy range of a few GeV to about 400 GeV are available. A complete data set is, however, available for p, π, and K projectiles at 100 GeV (lab) energy on p, C, Cu, Sn and Pb targets where the momenta of the secondary antiprotons are measured [150]. Apart from such data, some measurements on the $\bar{p}p$ and $\bar{p}C$ collisions in the sub-GeV to hundreds of GeV energy range are also available [172, 193, 206, 221, 275]. A semi-phenomenological fit to such data can, therefore, be employed for the calculation

of atmospheric $\bar{p}$ flux with some level of accuracy and this has been a popular approach [186, 191, 218–220] for more than twenty five years.

A precise estimation of the atmospheric $\bar{p}$ flux additionally requires reliable estimates for the secondary cosmic ray flux that may, in turn, produce further $\bar{p}$ by colliding with air nuclei. Tertiary $\bar{p}$s (arising from inelastically scattered secondaries) also contribute at low energies. One needs to further consider the residual galactic component of $\bar{p}$ in the case of very high (balloon) altitude.

4.2.2 Brief outline of various particle interaction models

In the string-based models, the high energy nucleonic interactions lead to the excitation of color flux tubes. Antiprotons are produced *via.* the decay of such color flux tubes and also in antiresonance decays; whereas, the $\bar{p}$ annihilation is modelled *via.* the annihilation of quark-antiquark pairs and the formation and subsequent decay of two color flux tubes with baryon number zero. The annihilation of baryon-antibaryon pairs proceeds in UrQMD according to rearrangement diagrams. Here, the formation of two $\bar{q}q$-strings of equal energies in the c.m. system is assumed, while the remaining constituent quarks are rearranged into newly produced hadrons.

At higher energies, the interactions of nucleons and nuclei are calculated on the basis of the Gribov-Regge theory [139] that describes the observed rise of cross-sections at high energies as a consequence of the exchange of multiple supercritical Pomerons [185]. All observed scattering processes are successfully described with the Reggeon-Pomeron scattering scheme [185]. Presently, the Gribov-Regge theory-based interaction models used for cosmic rays include the QGSJET 01c [94], VENUS 4.12 [106], DPMJET-III [132], NEXUS 3.97 [127, 128] and the EPOS 1.6 [107] models. Such different models in this class differ from each other in the details concerning the precise formulation of string formation and decay, treatment of the remnants etc. Apart from these a mini-jet model SIBYLL [88–90] is also available in CORSIKA. Some of these models are described briefly in *Chapter 3.*

4.3 Implementation of the simulations

In the present work, atmospheric cosmic ray proton and antiproton spectra are generated by employing the interaction models FLUKA 2008.3b and UrQMD 1.3 in the framework of the cosmic ray EAS simulation code CORSIKA (version 6.735) [202]. Following the default settings of the CORSIKA code, FLUKA and UrQMD have been used up to 80 GeV/n, while the model QGSJET 01c has been used above such energy threshold. As mentioned in Sec. 4.1, also use the high energy interaction models VENUS 4.12, NEXUS 3.97 and EPOS 1.6 is used, each in combination with the FLUKA model, to compare various theoretical estimates of the atmospheric $\bar{p}$ flux at energies beyond the BESS upper cutoff up to about 100 GeV. Other considerations/settings used in this work are briefly described in the following.

4.3.1 The primary spectra

Uncertainties in the determination of primary cosmic ray flux have been substantially reduced in recent years due to the precise measurements of such flux by the BESS-98 [50], BESS-TeV [201] and the AMS [179, 180] experiments. The observed total primary nucleon flux below 100 GeV/n is found to agree within an accuracy of 4.0% in the above three experiments [52, 199]. For such a reason, and considering the fact that our results would be compared with the BESS observations, the BESS-98 spectra is chosen as the input primary spectra in our simulations while extending the maximum (kinetic + rest-mass) energy of the primary particles up to 1 PeV/n. For reproducing the BESS-observed primary spectra in CORSIKA, the effect of solar modulation on the spectra has been handled by using the *force field approximation* [200, 210] in which the primary particle flux is expressed in terms of a time dependent *solar modulation potential* $\phi(t)$ that takes on different values for different epochs of solar activity [222]. For the BESS balloon-borne measurements of the atmospheric proton and antiproton fluxes in September 2001 at Ft. Sumner, USA [174, 175, 224], the primary cosmic ray spectra are generated by taking a solar modulation potential $\phi = 891$ MV [222] into account. Again, for the BESS sea-level measurements of the antiproton fluxes [224] at Tsukuba, Japan during 6th-11th May and 7th-13th December 1997, $\phi = 410$ MV [222] is considered as the mean value of the solar modulation potential.

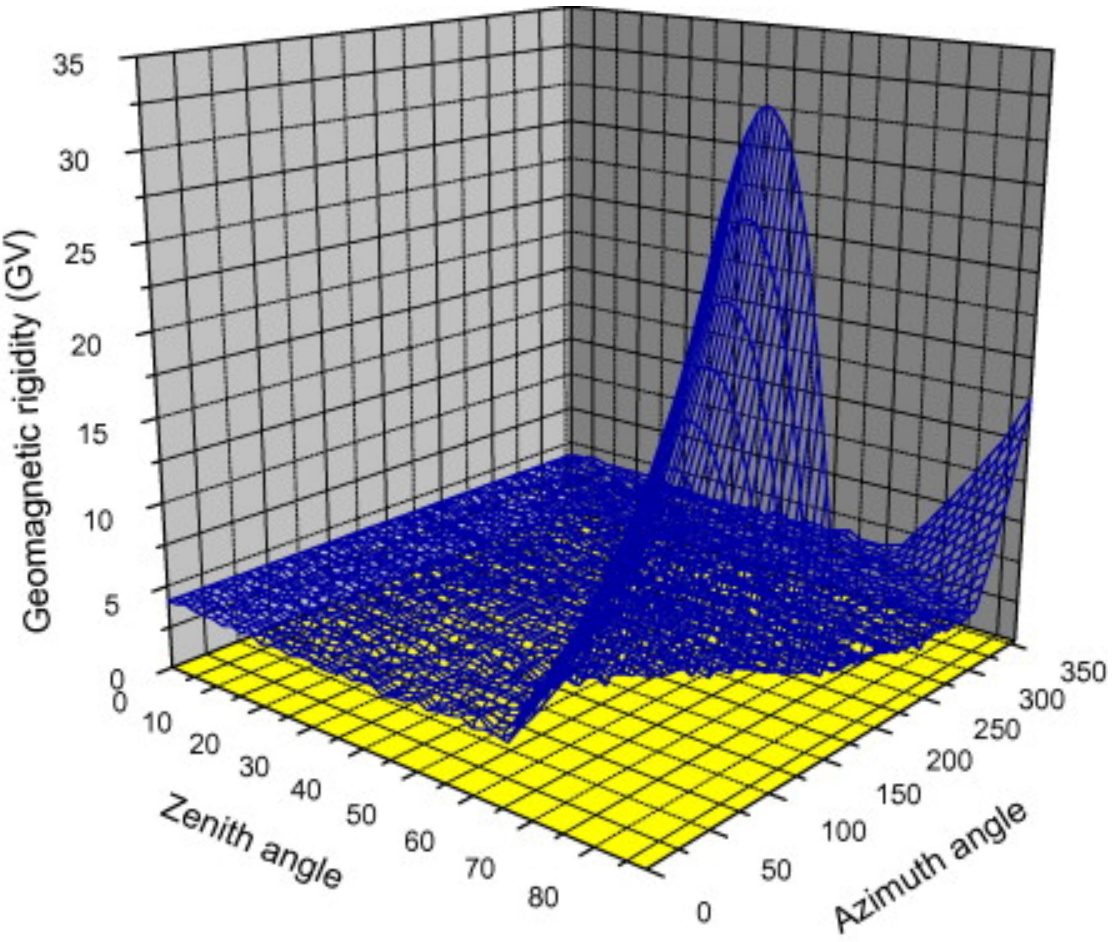

FIGURE 4.1: Directional dependence of the mean geomagnetic rigidity cutoff for primary cosmic rays at the location of Ft. Sumner, USA.

4.3.2 The geomagnetic rigidity cutoff

The geomagnetic rigidity cutoff calculations have been performed by using the (back) trajectory-tracing technique [216]. The quiescent International Geomagnetic Reference Field (IGRF) model of 1995 [215] for the Earth's magnetic field has been used for such calculations. Both the umbra and the penumbra regions in the rigidity range of a primary particle in any particular direction have been taken into consideration [189] in our treatment of the rigidity cutoff. In Figure 4.1, the values of the mean geomagnetic rigidity cutoff are displayed for the primary cosmic ray particles entering the atmosphere at the location of Ft. Sumner from various directions as an example of our rigidity calculations. Such cutoff calculations are used in the simulations to modify the primary cosmic ray spectra obtained from CORSIKA, although the calculation of the re-entrant albedo cosmic ray flux is not incorporated in the present simulations; see Section 4.5 below.

4.3.3 Other settings

The fluxes of cosmic ray particles also depend on the atmospheric density profile. Such a density profile, in turn, has latitudinal and seasonal variations. The effect of such variations on the atmospheric cosmic ray spectra is, however, expected to be small, particularly in the case of very high altitude observations. Therefore, the US-standard atmospheric model [209] with a planar approximationis considered in the present work.

Proton, helium and the heavier nuclei up to iron are considered here as the primary cosmic ray particles. Instead of taking each of the elements individually, the primary nuclei heavier than helium are taken in three separate groups, namely, medium ($5 < Z < 10, < A > \approx 14$), heavy ($11 < Z < 20, < A > \approx 24$) and very heavy ($21 < Z < 30, < A > \approx 56$) nuclei respectively [189]. The spectra for such groups are taken from the compilation of Reference [223]. The sum of the fluxes of individual elements in a group is taken as the flux of that particular group and the weighted average value of the power indices of such individual elements is taken as the power index of the group [189].

Particular care should, however, be taken for the simulation of atmospheric antiproton flux at a very high altitude. Such atmospheric antiprotons may, in fact, have significant contribution from the residual galactic $\bar{p}$s arriving at the observation level. In this work, a secondary $\bar{p}$ spectrum is generated by combining the simulation-generated (and normalized to the BESS-98 spectrum) primary proton spectrum with the recent measurement of antiproton to proton flux ratio obtained in the PAMELA experiment [170]. The resultant secondary $\bar{p}$ spectrum, adjusted for the location of Ft. Sumner and for a solar modulation potential appropriate for the BESS-2001 experiment, is considered along with the usual primary cosmic ray particles as the inputs in the simulations. However, the integrated secondary $\bar{p}$ flux is found to be only about $1.4 - 1.5\ 10^{-4}$ times the integrated primary proton flux in our simulations. It has been checked that such interstellar $\bar{p}$ flux, in fact, have negligible effects on the generated atmospheric antiprotons within the energy range considered by the BESS experiments and even beyond.

Note that the fluxes of atmospheric shower particles obtained by using CORSIKA have statistical as well as systematic errors. In the present work, nearly $4 - 20 \times 10^7$ events have been generated in each of our simulations for the estimation of the

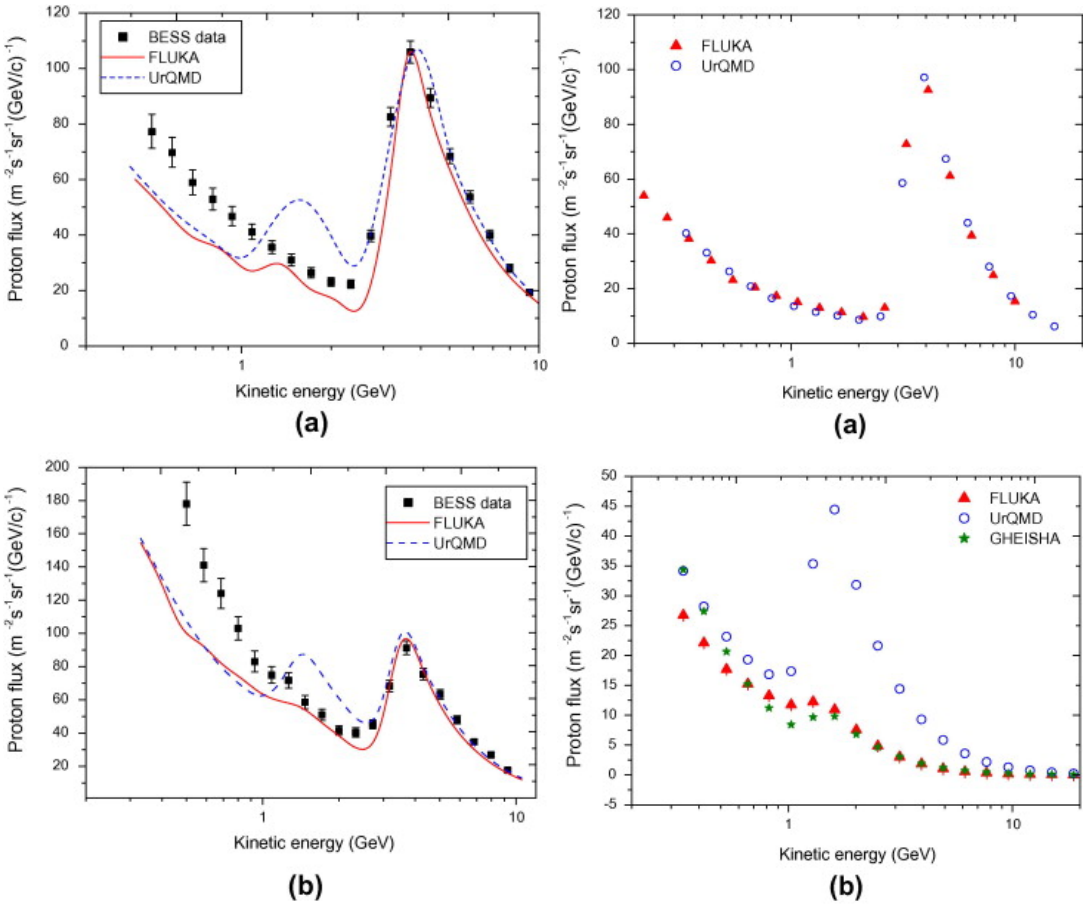

FIGURE 4.2: Left: Differential spectra of vertical atmospheric proton flux at the location of Ft. Sumner, USA that are obtained by using two hadronic interaction models at the atmospheric depths (a) 10.5 g cm^{-2} and (b) 26.4 g cm^{-2}. The results of the BESS-2001 observations at such depths [174, 175] are also given for comparison. Right: Contributions from (a) primary protons and (b) primary α particles to the simulated vertical secondary proton flux at an atmospheric depth 10.5 g cm^{-2} at the location of Ft. Sumner. The proton fluxes are generated by using various hadronic interaction models as indicated in the diagram.

fluxes of atmospheric shower particles, the results of which are presented in the following.

4.4 Simulated results and comparison with observations

The BESS-2001 experiment [174] is a balloon-borne experiment that was carried out in September 2001 at Ft. Sumner, USA. It consisted of a high resolution

spectrometer with a large acceptance capable of performing precise measurements of absolute fluxes of various cosmic rays and their dependence on the atmospheric depth. The secondary proton and helium spectra in an energy range $0.5 - 10.0$ GeV/n and the atmospheric muon spectra in a momentum range $0.5 - 10.0$ GeV/c were measured at atmospheric depths ranging from 4.5 to 28.0 g cm^{-2} during the slow descending period of the balloon flight [174, 175]. Atmospheric antiproton flux was also measured in the energy range $0.2 - 3.4$ GeV and, reportedly, at a mean atmospheric depth 10.7 g cm^{-2} [224]. The zenith angle θ_z of the BESS-2001 measurements was limited to $\cos\theta_z \geq 0.9$ to obtain nearly vertical fluxes of atmospheric particles [174].

The BESS experiment also measured the sea-level antiproton flux at KEK, Tsukuba during 6th-11th May and 7th-13th December 1997 at a mean atmospheric depth 994.0 g cm^{-2} in the energy range $0.2 - 3.4$ GeV [224].

Fig. 4.2 (left) depicts the simulated atmospheric proton flux at the location of Ft. Sumner at the atmospheric depths (a) 10.5 g cm^{-2} and (b) 26.4 g cm^{-2}. Corresponding BESS-measurements [174, 175] are also shown in the figure. It is noted that the statistical errors in the simulated spectra are quite small and fall within the widths of the representing lines in Fig. 4.2.

The BESS-2001-observed proton spectra in Fig. 4.2 (left) shows the following characteristic features. With the increase of energy from about 0.3 GeV, the differential flux initially decreases thus attaining a minimum value at about 2.5 GeV. Such a minimum is followed by an increase in flux up to a maximum at around 3.4 GeV above which the flux decreases again. Above about 2.5 GeV, bulk of the contribution to the observed flux is from primary protons with the peak being due to the geomagnetic cutoff effect. Below 2.5 GeV, the observed spectrum is due to secondary protons produced by the interaction of primary cosmic rays with atmospheric nuclei.

In Fig. 4.2 (left), it is found that the spectra derived from FLUKA and UrQMD models have features similar to those in the measured spectra. Both the models, however, yield fluxes that are lower than the measured values particularly at energies below 1.0 GeV. It is also noted that the simulated results match better with the measurements at 26.4 g cm^{-2} than at 10.5 g cm^{-2} in Fig. 4.2(left).

Fig. 4.2 (left) shows an additional peak in the UrQMD-derived spectrum at about 1.4 GeV. In this context, it is noted that the kinetic energy corresponding to the

mean vertical geomagnetic rigidity cutoff at Ft. Sumner [224] is also about 1.4 GeV/n for the threshold primary helium nuclei. To investigate if the anomalous peak in the UrQMD-derived flux in Fig. 4.2 (left) is due to such primary α particles, the separate contributions of (a) primary proton and (b) primary α components to the secondary proton flux are ploted in Fig. 4.2 (right) at an atmospheric depth 10.5 g cm^{-2} at the location of Ft. Sumner. It is clear from this figure that the additional peak in UrQMD in Fig. 4.2 (left) is indeed contributed by the primary helium nuclei. To check if there is any error in our simulations, the secondary proton flux from primary α particles is also computed in Fig. 4.2(b) (right) by using the GHEISHA model. It is found that no additional peak in the GHEISHA model, the result of which is consistent with the FLUKA result. Fig. 4.2 (right) thus seems to suggest that the fragmentation channel for quasi-elastic interactions between helium and air nuclei is overestimated in the UrQMD model. Such a finding is somewhat unexpected as the UrQMD model was primarily developed to address the nucleus-nucleus interactions and the model is known to well-reproduce the accelerator data. Further study on the stated feature in UrQMD seems, therefore, to be necessary. In Fig. 4.2, It is also noted that the results simulated with FLUKA and UrQMD models show very close agreement with each other at low energies, below about 1.0 GeV.

Fig. 4.3 shows the simulated atmospheric $\bar{p}$ fluxes in comparison with the BESS-measurements at balloon altitude, at mountain altitude and at the sea-level. The bandwidth of each of the bands displayed in this diagram represents the magnitude of statistical error in the simulations. At mountain altitude and at the sea-level, the $\bar{p}$ fluxes generated by UrQMD are found to be consistent with the BESS measurements within error bars. Such UrQMD-derived fluxes are, however, higher than the measured values at very high altitude. On the other hand, the FLUKA-generated fluxes are consistently higher than the measured values at all the atmospheric depths. The disagreement between the FLUKA-derived $\bar{p}$ spectra and the BESS observations is maximum at very high altitude and minimum at the sea level.

The results of our simulation for antiproton flux up to about 100 GeV at an atmospheric depth 10.7 g cm^{-2} is displayed in Fig. 4.4. To minimize statistical fluctuations, 40$-$50 million events are generated to obtain the flux from each model in this figure. The BESS measurements at Ft. Sumner [224] are also compared in Fig. 4.4. The fluxes generated by UrQMD + QGSJET and FLUKA + QGSJET

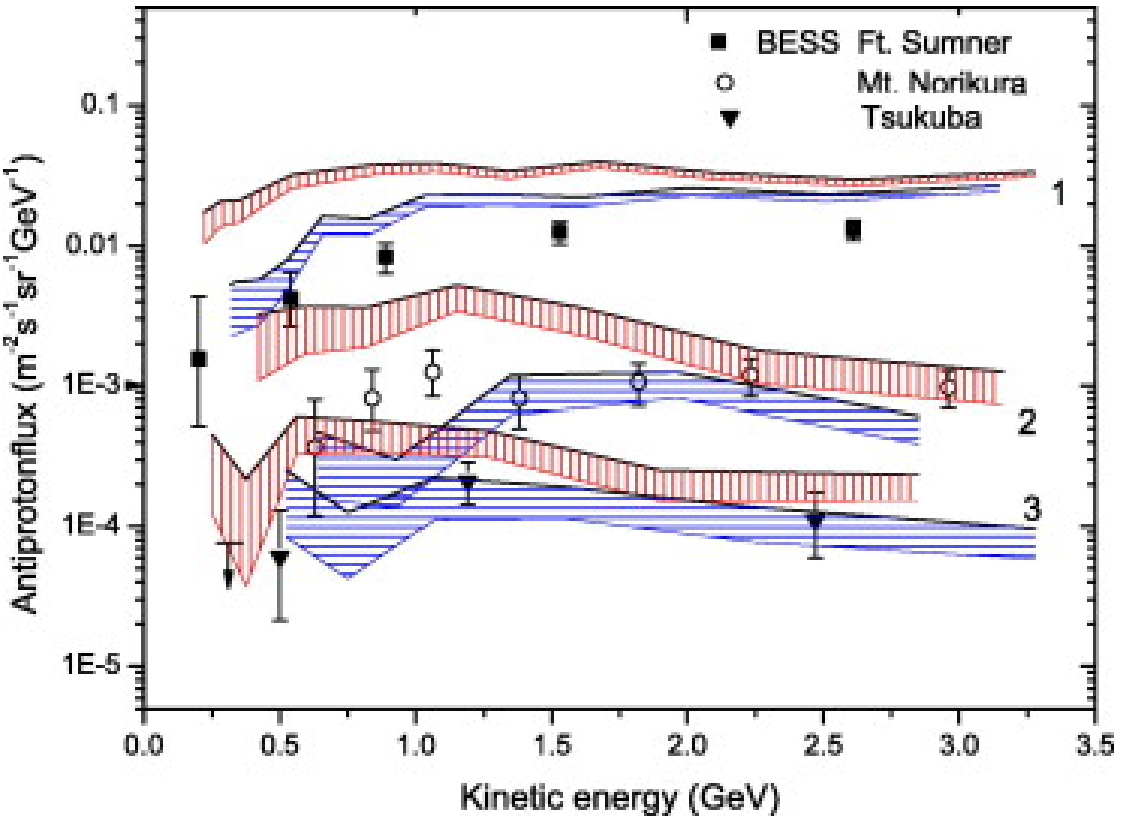

FIGURE 4.3: A diagram depicting the simulated differential spectra of vertical atmospheric antiprotons at multiple atmospheric depths. In this figure, the red (vertically striped) bands and the blue (horizontally striped) bands represent the results simulated with FLUKA and UrQMD models; whereas, the uppermost (marked by the numeral 1), middle (marked by the numeral 2) and the lowermost (marked by the numeral 3) pair of bands represent $\bar{p}$ fluxes at balloon altitude (at the location of Ft. Sumner, USA), at mountain altitude (Mt. Norikura, Japan) and at the sea-level (Tsukuba, Japan) respectively. Corresponding measurements by BESS-2001 [224], BESS-1999 [51] and BESS-1997 [224] experiments are also given for comparison. Note that the bands marked by the numeral 2 are obtained from our previous simulations [189].

combinations are found to differ significantly at the lower energy end; whereas, they predict nearly the same flux at higher (above about 5.0 GeV) energies. As we move to higher energies, the simulated $\bar{p}$ flux is increasingly influenced by the particle interaction characteristics at higher energies. It has been, so far, considered just a single model (QGSJET) for describing particle interactions above 80 GeV/n. It is, therefore, expected that the stated combinations of models will give nearly the same flux at such higher energies.

To probe further into the situations at energies ranging roughly from about 10 GeV to 100 GeV, additional sets of data are simulated by replacing QGSJET by

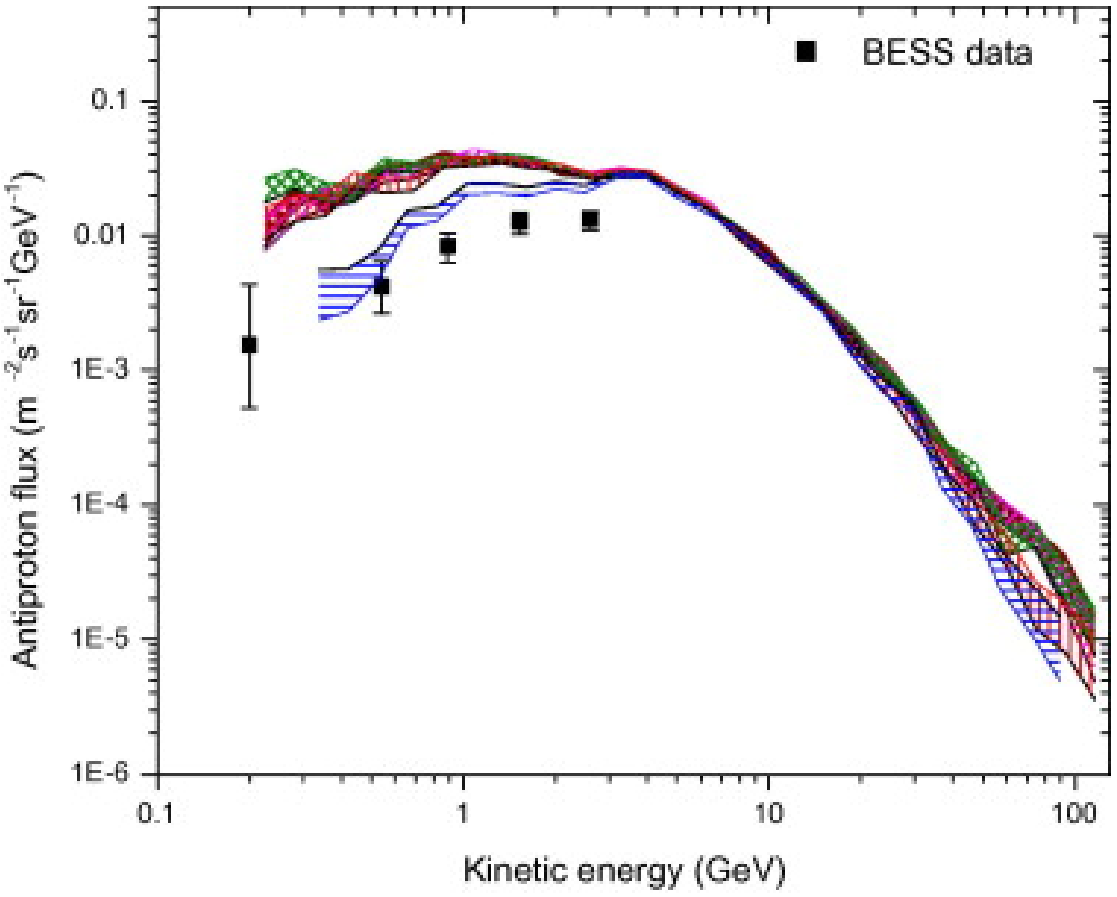

FIGURE 4.4: Atmospheric vertical antiproton flux simulated with UrQMD + QGSJET, FLUKA + QGSJET, FLUKA + VENUS, FLUKA + NEXUS and FLUKA + EPOS models at an atmospheric depth 10.7 g cm^{-2} at the location of Ft. Sumner, USA for the kinetic energy of antiprotons within a range $0.2 - 100$ GeV. Here, the blue (horizontally striped) band depicts the UrQMD + QGSJET combination, the red (vertically striped) band depicts the FLUKA + QGSJET combination, the magenta band (shaded by right-tilted lines) represents the FLUKA + NEXUS combination, the green (cross-hatched) band represents the FLUKA + VENUS combination and the brown (square-hatched) band represents the FLUKA + EPOS combination. Fluxes obtained by the BESS-2001 observation are also given for comparison.

VENUS, NEXUS and EPOS interaction models to describe particle interactions above 80 GeV/n, while continuing with FLUKA below 80 GeV/n. The spectra obtained from such combinations are also shown in Fig. 4.4. In the absence of any experimental data, the merit of the VENUS, NEXUS or the EPOS model could not be judged over the QGSJET model as far as the $\bar{p}$ production in the atmosphere is concerned. It is, however, clear from the comparison of $\bar{p}$ fluxes in Fig. 4.4 that the theoretically predicted antiproton flux has strong dependence on

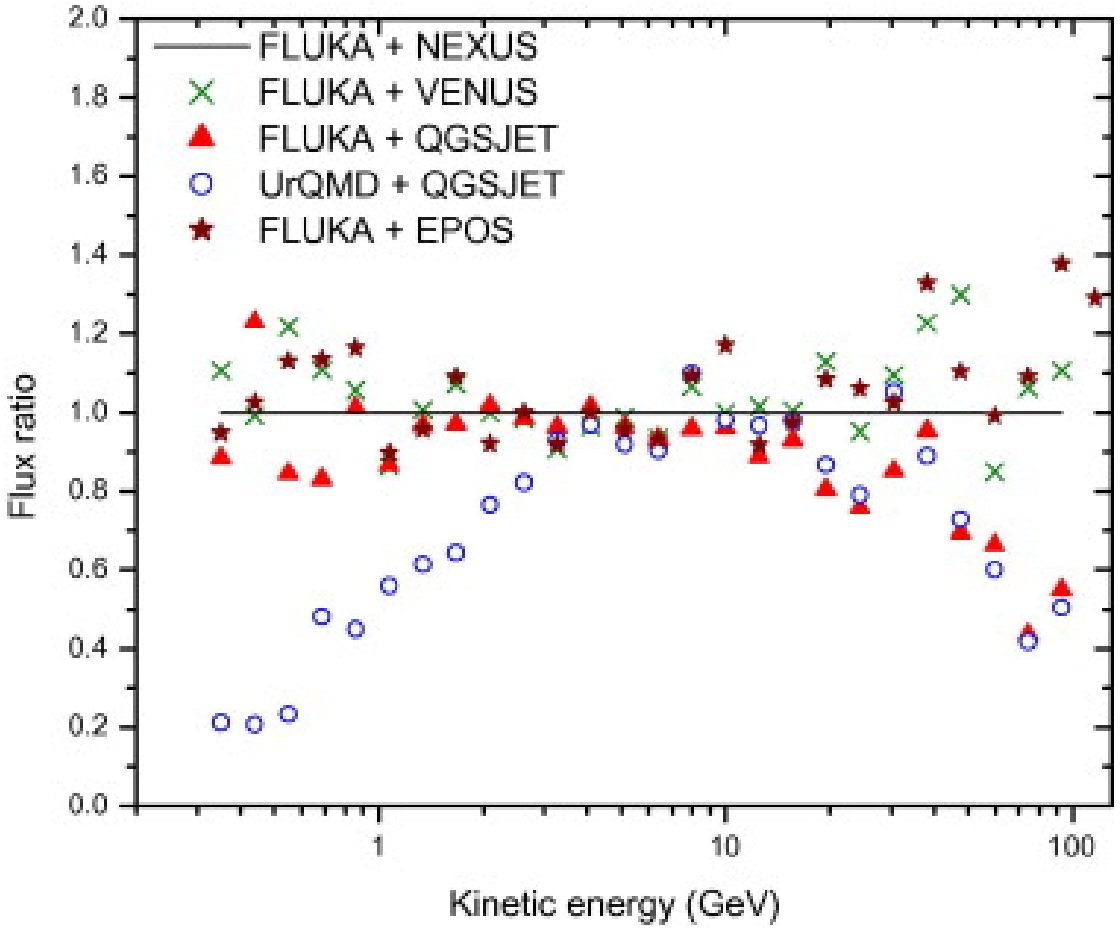

FIGURE 4.5: Ratios of the mean atmospheric antiproton fluxes simulated with each of the FLUKA + QGSJET, FLUKA + VENUS, FLUKA + EPOS and the UrQMD + QGSJET combinations to the ones simulated with the FLUKA + NEXUS model for various values of kinetic energy of the antiprotons at a mean atmospheric depth 10.7 g cm^{-2} at the location of Ft. Sumner, USA.

high energy interaction models over the energy range considered here.A characteristic feature of the atmospheric antiproton spectrum is that it peaks at around 2 GeV, decreasing rapidly towards lower energies, that is reflected in the simulated spectra as displayed in Fig. 4.4. Such a feature is not clearly visible in the BESS atmospheric observations because of the limited energy range of the experimental spectra.

To quantify the uncertainties in the theoretical $\bar{p}$ fluxes to a certain extent, the ratios of average $\bar{p}$ fluxes predicted by each of the FLUKA + QGSJET, UrQMD + QGSJET, FLUKA + VENUS and the FLUKA + EPOS combinations to the average fluxes obtained from the FLUKA + NEXUS combination (arbitrarily chosen as reference for the comparison) is plotted that are displayed in Fig. 4.5. While

such ratios are found to be close to unity in the energy range around $3 - 10$ GeV for all the models, they significantly deviate from each other at higher energies. The flux-ratios even show more than 60% variation for different models at energies around 100 GeV. In Fig. 4.5, it is found that the QGSJET-predicted mean flux at kinetic energies above about 10 GeV is substantially lower than those predicted by the NEXUS or the VENUS model. The EPOS 1.6 model follows a trend similar to that shown by VENUS at such high energies. Below about 3 GeV, the UrQMD model gives appreciably lower fluxes than those obtained by the FLUKA model as was already noted in Fig. 4.4. Possibilities of statistical fluctuations are, of course, present in such results, but such systematic deviations as depicted in Fig. 4.5 can not be accommodated in terms of statistical fluctuations.

Since all the interaction models used here are appropriately tuned to the results obtained from the known collider and other experiments, the difference between the predictions of such models are mainly due to our limited understanding of high energy particle interactions.

4.5 Summary and Discussion

Atmospheric proton and antiproton fluxes at different atmospheric levels are calculated in this article by using MC simulations with different particle interaction models and compared to the BESS experimental results. For spectra below about 10 GeV, corresponding to the experimental measurements, only the interaction models FLUKA and UrQMD are relevant. Here, it is further extend our study of the atmospheric $\bar{p}$ flux up to 100 GeV where the high energy particle interaction models QGSJET 01c , VENUS 4.12, NEXUS 3.97 and EPOS 1.6 start to influence the simulated flux. As a consequence, it can be examined the effect of such interaction models on the calculated $\bar{p}$ spectra in this article. The results of such study lead to the following observations.

1. It is interesting to note that the predictions of $\bar{p}$ fluxes obtained from FLUKA and UrQMD show significant deviations from each other, particularly at energies below about 3 GeV.

The model UrQMD presents reasonable description of the BESS $\bar{p}$ data at mountain altitude and at sea level; whereas, it overestimates the antiproton flux at very high altitude thus possibly indicating that there is an enhanced production of $\bar{p}$ followed by an enhanced annihilation in this particular model. Such an enhanced production of $\bar{p}$ in UrQMD may not be entirely unexpected as the model yields a higher multiplicity in comparison with the fixed target experiments.

The fact that FLUKA consistently yields a higher $\bar{p}$ flux than the measurements at all the observation levels possibly indicates a strongly enhanced $\bar{p}$ production in this model unless It is assumed that the BESS experiments have missed a sizable $\bar{p}$ events. The latter possibility is, however, thin as the fluxes obtained from UrQMD is consistent with the measured fluxes at sea-level and at mountain altitude. Atmospheric $\bar{p}$ annihilation also appears to be slightly enhanced in the FLUKA model as the disagreement between the FLUKA-generated $\bar{p}$ spectra and the ones obtained from the BESS measurements is found to decrease with increasing atmospheric depth.

As mentioned in Sec. 4.2, FLUKA mainly exploits the DPMJET-III model in describing high energy nucleon-nucleus interactions. DPMJET-III is known to moderately reproduce the energy dependence of antiproton to proton ratio at $y_{cm} = 0$ in proton-proton collisions as measured in the accelerator experiments [190]. It also reproduces the BRAHMS findings (from the RHIC experiment) regarding the dependence of antiproton to proton ratio on cms rapidity practically within experimental errors [188]. Although the consistency of the model parameters can not be checked in the energy range relevant for the present study as there is no direct experimental data on antiproton rapidity distribution in collisions with air or similar targets, the disagreement between the FLUKA-based fluxes and the measured fluxes on such a scale as noticed in the present study is, nevertheless, not an expected one.

It is worthwhile to note that the $\bar{p}$ flux obtained by Stephens [220] through a three dimensional MC simulation within a phenomenological framework was also found to be substantially higher in comparison with the BESS-observed flux at balloon altitude and in comparison with the theoretical unidirectional flux. Stephens [220] ascribed such a discrepancy to the use of the global spectra of primary cosmic ray particles instead of those observed by the BESS experiments. Such a possibility seems to be unlikely as the difference

between the measured flux and the theoretically predicted flux is rather large in this particular case. As mentioned earlier, the balloon in the BESS-2001 experiment at Ft. Sumner was initially floated at an atmospheric depth 4.5 g cm^{-2} from where it started to descend slowly to an atmospheric depth of around 30.0 g cm^{-2} before the termination of the experiment [224]. In the absence of any knowledge regarding the effective observation time at each atmospheric depth, the $\bar{p}$ flux at balloon altitude is computed in the present investigation (and in [220]) at 10.7 g cm^{-2} that was the mean atmospheric depth for the BESS-2001 experiment. As the $\bar{p}$ flux in the atmosphere does not vary linearly with the atmospheric depth, such an inability to precisely determine the atmospheric depth could be at least one of the possible reasons for the difference between the simulated and the measured fluxes at the balloon altitude.

It is here noted that a few phenomenological MC simulations yield $\bar{p}$ fluxes that are consistent with the BESS observation at balloon altitude except below 1.0 GeV unless it is assumed that the tertiary antiprotons do not loose their energy in collisions with atmospheric nuclei [224]. Notwithstanding such assumptions, none of the above simulations consistently describe the BESS measurements of $\bar{p}$ spectra at all the observation levels. The present study, on the other hand, seems to suggest that the BESS observations of $\bar{p}$ spectra are relatively well described by the UrQMD model.

2. The results presented in this article show a significant discrepancy between the BESS-observed secondary proton spectra at very high altitude below the geomagnetic rigidity cutoff and the ones obtained from the interaction models FLUKA and UrQMD, particularly at the low energy part of the observed spectra. It is worth noting here that the re-entrant albedo particles, a consideration of which has been left out of the present investigation, are unlikely to be the cause of such a difference between the measured and the simulated flux of the secondary protons. This is because of the fact that the flux of such re-entrant albedo protons, as measured by the AMS experiment [182], is smaller by more than an order in comparison with the BESS-observed secondary proton flux below the geomagnetic cutoff till down to at least 0.3 GeV. It is also noted that the BESS collaboration (see the footnote in Ref. [174]) found no such re-entrant albedo proton flux in their observation at the balloon altitude.

The difference that is found between the simulated and the observed proton spectra at very high altitude is in apparent contradiction with the results of our earlier simulations [189] that display reasonable agreement with the BESS-observed proton flux at mountain altitude. Fig. 4.2 in Sec. 4.4, however, demonstrate that the model-predicted proton fluxes at a lower altitude are indeed closer to the observed proton fluxes in comparison with those at a higher altitude. It may be thus inferred from the above results that the BESS observations seem to favour a higher production rate of protons in the nucleon-air collisions than the ones implemented in the FLUKA and the UrQMD models. It is, however, noted that the results of a single experimental measurement may contain uncertainties so that further observations of cosmic ray proton fluxes at multiple altitudes, along with the corresponding MC simulations, may be required to arrive at a definite conclusion on this particular issue.

3. The recent findings of the PAMELA experiment on positron excess [171, 177] but no antiproton excess [170] in the energy range from sub-GeV to about 180 GeV lead to a nontrivial constraint on dark-matter models that try to account for the positron excess [194, 204, 208]. In the stated findings, the excess is determined by comparing with the background predictions from cosmic ray propagation models. The background $\bar{p}$ spectrum, that originates from the hadronic production induced by cosmic rays on the ISM, is generally calculated with the GALPROP numerical propagation code either by applying the parametrization of the invariant $\bar{p}$ production cross-section [211] or by implementing the DTUNUC MC code [217]. Uncertainties in $\bar{p}$ flux due to the uncertainties in nuclear parameters, that are estimated from the parametrization of the maxima and the minima of the measured inclusive $\bar{p}$ cross-sections in hadron-hadron and hadron-nucleus collisions, were found earlier to be about $22 - 25\%$ [195]; whereas, the uncertainties in the nuclear parameters of the DTUNUC program, that essentially rests on the DPM model, were estimated to be about 40% [217].

   The present study also indicates, albeit indirectly, that the theoretical galactic $\bar{p}$ spectrum may contain large uncertainties due to the uncertainties in our knowledge of the particle interaction characteristics. Our investigation shows that at energies below about 3 GeV, the BESS observed atmospheric antiproton fluxes, at an atmospheric depth roughly comparable to the depth traversed by the cosmic rays in the Galaxy, are substantially lower than

those obtained with the model FLUKA that may be regarded as a DPM class of model. At energies above about 10 GeV, the model predictions cannot be tested experimentally but, importantly, the predictions from different popular microscopic high energy interaction models tend to differ appreciably. In this context, it can be noted that the model EPOS is known to produce more baryons/antibaryons in comparison with most of the other models including QGSJET that seems to be reflected in our results; see Figs. 5 and 6 in Sec. 4.4. Our investigation in Fig. 4.5, in fact, suggests that the amount of uncertainty between different model predictions is not the same at all energies. Around 300 MeV, such uncertainity is as large as 80% that reduces substantially towards higher energies, particularly above about 3 GeV. Above 10 GeV, the uncertainity, however, increases again with energy and even becomes more than 60% at about 100 GeV. In the near future, to take up a further investigation on the secondary antiproton spectrum is planned by extending the maximum kinetic energy of such antiprotons to about 180 GeV or even beyond and by exploiting the updated versions of high energy interaction models, such as the QGSJET-II [212, 213] and the EPOS 1.99 [149] models, in the framework of CORSIKA 6.980 (along with FLUKA 2011.2 to simulate below 80 GeV/n) for a better understanding of the recent PAMELA observations [171]. It may also be important here to note that the proposed measurements of $p + C \rightarrow \bar{p}$ and $\pi + C \rightarrow \bar{p}$ by the NA61/SHINE fixed-target experiments [176, 183] at a few hundred GeV (lab) energy is expected to assist us in improving our understanding on the production of antiprotons thereby resolving the noted discrepancies between the interaction models in near future.

Finally, it may be argued that the magnitude of uncertainties quoted in the theoretical calculations of $\bar{p}$ flux, that are obtained by employing semi-phenomenological fit to the experimental data, should perhaps be taken with some caution. This is because of the fact that the errors in the experimental results, based on which the model parameters are fitted or parametrized, are often underestimated or overlooked that may, in turn, affect the entire theoretical prediction. Well known examples are the inelastic $p - \bar{p}$ cross-sections that were measured by three different experiments at FERMILAB and the values at $\sqrt{s} = 1800$ GeV were found to vary from 80.03 ± 2.24 mb to 71.71 ± 2.02 mb [173, 181, 184]. Therefore, it is obvious that the model parameters that were tuned in accordance with the earlier quoted

experimental $p - \bar{p}$ cross-sections would suffer from additional uncertainties. Thus, the consistencies of the predictions of a model in different circumstances may alone provide the validity of its inputs. In view of the results of the present analysis, a detailed study of the galactic $\bar{p}$ flux by exploiting different microscopic interaction models seems to be worth pursuing in the context of the PAMELA observation and its interpretation in terms of the standard/non-standard (dark matter etc.) sources.